Analytical Localization Lengths in an One-Dimensional Disordered Electron System

Alexander Rauh

Institut für Physik, Carl von Ossietzky Universität Oldenburg, D-26111 Oldenburg, Germany

Reprint requests to A. R.; E-mail: alexander.rauh@uni-oldenburg.de

Z. Naturforsch. **64a,** 205 – 221 (2009); received May 21, 2008 / revised August 26, 2008

Analytical approximations of the Lyapunov exponent are derived for a random displacement model with equal potential barriers and random positions of the scatterers. Two asymptotic regions are considered corresponding to high and low reflectivity of the single scattering potential. The analytical results are in terms of a distribution function W for certain phases of the transfer matrices. A functional equation for W is derived and numerically solved. This serves to validate the analytical asymptotic formulas which turn out to be accurate in the high and low reflectivity regions with dimensionless wave number $K < 2$ and $K > 6$, respectively. The high wave number asymptotics allows for an analytical examination of the sufficient conditions for Anderson localization.

Key words: Anderson Localization; Lyapunov Exponent; Transfer Matrix; Functional Equation.
PACS numbers: 71.23.An

1. Introduction

The present interest in one-dimensional disordered electron systems is mainly focused on the effect of correlated disorder, see e. g. [1 – 4], on Anderson localization in Bose-Einstein condensates [5], or on the effect of dynamic disorder as by phonons [6]. In this paper, we give an exemplary direct insight into the properties of a random system by deriving analytical expressions of the Lyapunov exponent. This is achieved for asymptotic regions of high and low reflectivity of a single scatterer. The present contribution is thus complementary: (i) to the deep existence theorems of mathematical spectral theory, for an overview see e. g. [7, 8], including Anderson's seminal paper [9] which contains a highly nontrivial convergence proof of a perturbation series; (ii) to scaling theory, see e. g. [10 – 12]; (iii) to numerical studies, see e. g. [13 – 18]. Our model allows for arbitrary disorder, in contrast to other analytical studies: (i) on the Lloyd model [19, 20], where disorder is confined to a Cauchy distribution; (ii) like [21], which is limited to weak disorder; (iii) on the random dimer model [4], which deals with a binary alloy with a discrete distribution. As will be seen, the requirement of positive Lyapunov exponents will restrict, to some extent, the set of permitted disorder distributions.

We adopt a random displacement model (RDM) which is characterized as follows: There are N equal repellent scatterers with nonoverlapping potentials at random positions $d_n(\varepsilon_n) = (n + \varepsilon_n)\, d$, where the random numbers ε_n, $n = 1, 2, \ldots N$, are statistically independent and equally distributed by a distribution function $p(\varepsilon)$. The Hamiltonian of the RDM has "almost surely a dense pure point spectrum with exponentially decaying eigenfunctions" [22].

The free electron regions between two neighbouring scattering potentials are characterized by the amplitudes $\{a_n, b_n\}$. Since eventually we are interested in localized states, which have zero particle current density, the amplitude ratio, $a_n/b_n = \exp[\mathrm{i}\varphi_n]$, lies on the unit circle. The disorder distribution $p(\varepsilon)$ induces a distribution function $W(\varphi)$ of the phases φ_n, and W will fully characterize localization or delocalization. We have to assume that W exists in the limit of infinitely many scatterers, and that this function is the same for almost all displacement configurations $\varepsilon_1, \varepsilon_2, \ldots$.

According to the Oseledec-Ruelle theorem, see e. g. [7], the asymptotic behaviour, $|x| \to \infty$, of the solution of the stationary Schrödinger equation with stochastic potential $q_\omega(x)$,

$$-\frac{\hbar^2}{2m}\psi''(x) + q_\omega(x)\psi(x) = E\,\psi(x), \quad x \in \mathbf{R},$$

either grows or decays exponentially for almost all disorder configurations provided certain conditions of the potential q and of the distribution function of the disor-

der parameter space ω are fulfilled. We will specify the conditions for the RDM in Section 6. The asymptotic behaviour, in principle, depends on the initial condition at $x = x_0$ and on the energy E of the 2×2 transfer matrix $M(x,x_0;E)$ which enters when the stationary Schrödinger equation is considered as a dynamical system:

$$\begin{pmatrix} \psi(x) \\ \psi'(x) \end{pmatrix} = M(x,x_0;E) \begin{pmatrix} \psi(x_0) \\ \psi'(x_0) \end{pmatrix}.$$

Because the Wronskian is constant, M has determinant 1. As a consequence, the two eigenvalues $\mu_{1,2}$ of M have the property $\mu_1\mu_2 = 1$, and if μ_1 exponentially increases with $|x| \to \infty$, then μ_2, being the inverse of μ_1, decreases exponentially. Moreover, if $\boldsymbol{\nu}_0 = (\psi(x_0), \psi'(x_0))$ is any initial vector, then $M\boldsymbol{\nu}_0 \to$ const. $\mu_1 \mathbf{e_1}$ almost always; exception is when $\boldsymbol{\nu}_0$ is parallel to the eigenvector $\mathbf{e_2}$ of the exponentially decreasing eigenvalue μ_2. Only these exceptional cases lead to physically acceptable states. Boundary conditions at x_0, which are necessary for self-adjoinedness (e. g. in the limit $x_0 \to -\infty$), lead to discretization of the energy E_n, $n = 1,2,\ldots$. Thus, if the point spectrum lies in the interval $E \geq 0$ and the stochastic potential for $|x| \to \infty$ typically leads to expontially increasing eigenvalues μ_1 in the energy interval $E \geq 0$, then the bound states at $E = E_n$ are exponentially localized according to $\mu_2 \equiv 1/\mu_1$. Obviously, the localization length at $E = E_n$ can be inferred, almost always, from the asymptotic behaviour of $\|M(x,x_0 : E_n)\boldsymbol{\nu}_0\|$ starting with any initial state $\boldsymbol{\nu}_0$ without regard to boundary conditions.

We remark that an analogous situation can be observed also for determistic one-dimensional Hamiltonians. For instance, in the case of the harmonic oscillator, the amplitude $\|\boldsymbol{\nu}\| = \|M(x,x_0;E)\boldsymbol{\nu}_0\|$ exponentially increases for almost all initial vectors $\boldsymbol{\nu}_0$; this implies that the bound states are localized with the negative exponent. As is well known, the (asymptotically leading) exponent is proportional to x^2, whereas random systems give rise to an asymptotic exponent linear in $|x|$, in general. As another deterministic example, the radial part of the wave function of the hydrogen atom behaves asymptotically proportional to $\exp[+|\text{const.}|\, r]$, $r = \sqrt{x^2+y^2+z^2} > 0$ for most initial conditions, whereas the bound states are proportional to $\exp[-|\text{const.}|\, r]$ to leading order.

The Lyapunov exponent characterizes the asymptotic behaviour of the wave function $\psi(x)$ in the limit of large $|x|$. For the RDM, this exponent will be defined in terms of the free electron amplitudes $A_n = \sqrt{|a_n|^2 + |b_n|^2}$ in the limit $n \to \infty$.

In the high energy limit, our asymptotic analytical formulas are numerically corroborated for wave numbers $wK > 6$, where K corresponds to the energy $E(K) = \hbar^2/(2m)K^2$, and w is the width (support) of a single scatterer potential [the energy scale is fixed by the potential strength $V = \hbar^2/(2m)K_V^2$; we chose mostly $wK_V = 3.2$]. Similarly, the low energy asymptotics is approximately validated for $wK < 2$. However, this region is less intriguing for Anderson localization, because simply no bound state may fall into this domain. The checks are performed by means of a functional equation for the distribution $W(\varphi)$ which we solve numerically to high accuracy; it is derived in Appendix C.

The paper is organized as follows. In the next section we briefly outline the transfer matrix formalism and define the Lyapunov exponent for the model. In Section 3 we derive a recurrence relation for the phases φ_n and connect it with the Lyapunov exponent. Section 4 introduces the distribution $W(\varphi)$ for the problem, and connects this function to a cumulative distribution, which obeys a linear integral equation. Some computer runs with direct simulation of the transfer phases are displayed and compared with the numerical solution of the integral equation. In Section 5 the integral equation is solved perturbatively up to third order of the reflection coefficient ρ. The Lyapunov exponent, derived from the perturbative solution, is of second order in ρ with first- and third-order terms vanishing exactly. The result gives the correct zero value of the Lyapunov exponent in the limit of a regular lattice. In Section 6, we discuss the dependence of the asymptotic Lyapunov exponent on the disorder distribution $p(\varepsilon)$. The low energy asymptotics is derived in Section 7 from the recurrence system. There follow four appendices. In Appendix A, we outline the computer code to solve numerically the functional equation for $W(\varphi)$. In Appendix B formulas are proved, which are used in the main text and also in Appendix C and D, where, respectively, the functional equation for $W(\varphi)$ is derived, and $W_{\text{reg}}(\varphi)$ of a regular lattice is explicitly given.

2. Transfer Matrix and Lyapunov Exponent

The random displacement model [22] is characterized by equal, spin-independent, potential barriers with

distances

$$d_n = (n+\varepsilon_n)\,d, \quad n = 1,2,\ldots N, \tag{1}$$

from the origin. The ε_n are independent random numbers with the identical distribution function $p_n(\varepsilon_n) \equiv p(\varepsilon)$. The latter has finite support with $p(\varepsilon) = 0$ for $|\varepsilon| > \varepsilon^*$, and to avoid overlapping, one requires that $\varepsilon^* < 1/2(1-w/d)$, where w is the width (support) of a single barrier and d the mean spacing; clearly $w < d$. In illustrations, we will mostly assume the constant distribution

$$p(\varepsilon) = \Theta(\varepsilon^* - |\varepsilon|)/(2\varepsilon^*), \tag{2}$$

where $\Theta(x) = 1$ for $x > 0$, and $\Theta(x) = 0$ else, is the Heaviside function. The regular case is obtained by setting all $\varepsilon_n = 0$, which is equivalent to $p(\varepsilon) = \delta(\varepsilon)$.

In the potential-free regions the electron state $\psi(x)$ is described (we omit spin indices) by the amplitude vectors $\mathbf{A}_n = \{a_n, b_n\}$. Defining $\varepsilon_0 := 0$, $d_0 := -w/2$, $d_{N+1} := L + w/2$, and $\mathrm{i} := \sqrt{-1}$, we write in the interval $0 \le x \le L$

$$\begin{aligned} &\psi(x) = a_n \exp[\mathrm{i}Kx] + b_n \exp[-\mathrm{i}Kx], \\ &d_n + w/2 < x < d_{n+1} - w/2, \quad n = 0,1\ldots N. \end{aligned} \tag{3}$$

The corresponding energy is $E(K) = \hbar^2 K^2/(2m)$. Consecutive amplitude vectors are connected through 2×2 transfer matrices T_n:

$$\mathbf{A}_n = T_n \mathbf{A}_{n-1}, \quad \mathbf{A}_N = T^{(N)}\mathbf{A}_0, T^{(N)} = T_N T_{N-1}\ldots T_1. \tag{4}$$

Constancy of the particle current density

$$\begin{aligned} j(x) &= \frac{\hbar}{2m\mathrm{i}}\left[\psi^*(x)\frac{\mathrm{d}\psi(x)}{\mathrm{d}x} - \psi(x)\frac{\mathrm{d}\psi^*(x)}{\mathrm{d}x}\right] \\ &= \frac{\hbar K}{m}(|a_n|^2 - |b_n|^2), \quad n = 0,1,\ldots, \end{aligned} \tag{5}$$

(or equivalently of the Wronskian) implies that for all $n = 1,2\ldots N$

$$\det(T_n) = \det(T^{(N)}) = 1. \tag{6}$$

The definition of the Lyapunov exponent Λ, used here from [23], takes into account the dependence on the initial amplitude vector $\mathbf{A}_0$:

$$\begin{aligned} &\Lambda(\mathbf{A}_0) = \overline{\lim}_{N\to\infty}\frac{1}{N}\ln(A_N), \\ &A_N \equiv \|\mathbf{A}_N\| = \sqrt{|a_N|^2 + |b_N|^2}. \end{aligned} \tag{7}$$

In the adopted model, the T_n are independent, identically distributed random matrices, which are the basic prerequisites of existence theorems on Λ, see e. g. [23 – 25].

We write the transfer matrix of a scatterer located in the coordinate origin as

$$T_0 = \begin{pmatrix} 1/t^* & -r^*/t^* \\ -r/t & 1/t \end{pmatrix}, \tag{8}$$

where t and r are the transmission and reflection coefficients, respectively, and the star denotes complex conjugation. The polar form reads

$$\begin{aligned} &t = \tau\exp[\mathrm{i}\theta], \quad r = \rho\exp[\mathrm{i}(\theta+\sigma)], \\ &\tau^2 + \rho^2 = 1. \end{aligned} \tag{9}$$

In the case of scatterers with inversion symmetry, the phase $\sigma \equiv \sigma(K) = \pm\pi/2$; sign changes occur at wave numbers K, where $\rho(K) = 0$. The matrix T_n, which corresponds to the scatterer at position d_n, is obtained from T_0 by translation:

$$\begin{aligned} &T_n = (U_n)^{-1} T_0 U_n, \\ &U_n = \begin{pmatrix} \exp[\mathrm{i}K\,d_n] & 0 \\ 0 & \exp[-\mathrm{i}K\,d_n] \end{pmatrix}. \end{aligned} \tag{10}$$

It is convenient to introduce the unitarily equivalent amplitude vectors

$$\mathbf{A'}_n = U_n \mathbf{A}_n, \tag{11}$$

which transform $T_n \to M_n$ with

$$M_n = T_0 U_n (U_{n-1})^{-1}, \quad n = 1,2,\ldots N, \quad U_0 = 1. \tag{12}$$

For the rest of this paper, the prime of $\mathbf{A'}_n$ will be omitted. In the regular case with $d_n = n\,d$, the matrices $M_n \equiv M_1$ are the same for all n.

For illustration, let us determine the Lyapunov exponent for the regular case. As compared with T_0, the matrix M_1 contains the additional phase shift $\alpha = K\,d$ picked up by the state when the electron proceeds to the neighbouring scatterer:

$$\begin{aligned} &M_1 = \begin{pmatrix} \frac{1}{\tau}\exp[\mathrm{i}(\theta+\alpha)] & -\frac{\rho}{\tau}\exp[-\mathrm{i}(\sigma+\alpha)] \\ -\frac{\rho}{\tau}\exp[\mathrm{i}(\sigma+\alpha)] & \frac{1}{\tau}\exp[-\mathrm{i}(\theta+\alpha)] \end{pmatrix}, \\ &\alpha = K\,d. \end{aligned} \tag{13}$$

The eigenvalues $\mu_{1,2} \equiv \mu_{1,2}(K)$ of M_1 are determined from the trace $S \equiv S(K)$ and the condition that $\det(M_1) = 1$:

$$S \equiv \mu_1 + \mu_2 = 2\frac{\cos(\theta+\alpha)}{\tau}, \quad \mu_1\,\mu_2 = 1. \tag{14}$$

If $S^2 < 4$, then the eigenvalues $\mu_{1,2} = \exp[\pm i\lambda]$ lie on the unit circle; this corresponds to band energies in the case of an infinite or periodic lattice. If $S^2 > 4$, then the eigenvalues $\mu_{1,2} = \exp[\pm\lambda]$ are real with one of them, say μ_1, larger than 1. We write the initial amplitude vector in terms of the eigenvectors $\mathbf{e}_{1,2}$ of M_1:

$$\mathbf{A}_0 = c_1\mathbf{e}_1 + c_2\mathbf{e}_2, \tag{15}$$

and obtain

$$A_n = \|(M_1)^n\mathbf{A}_0\| = \|c_1\mu_1^n\mathbf{e}_1 + c_2\mu_2^n\mathbf{e}_2\|. \tag{16}$$

Clearly, if the eigenvalues $\mu_{1,2}$ lie on the unit circle, then A_n is bounded for any integer n. According to the definition (7), the Lyapunov exponent $\Lambda = 0$ for arbitrary initial amplitudes $\mathbf{A}_0$. On the other hand, if $S^2 > 4$, which corresponds to energies in a band gap, we have

$$\lim_{n\to\infty} A_n = \text{const. } \exp[n\lambda], \quad \lambda > 0, \tag{17}$$

which gives rise to $\Lambda(\mathbf{A}_0) = \lambda$ for almost all initial amplitudes; exception is $\mathbf{A}_0 = c_2\mathbf{e}_2$, where $\Lambda = -\lambda$. The special case $S^2 = 4$ corresponds to band edges and is singular with degenerate eigenvalues $\mu_1 = \mu_2 = \pm 1$.

3. Recurrence Relations

Similarly to [26], where a random Kronig-Penney model was studied, we start with the amplitude ratio

$$a_n/b_n = \exp[i\varphi_n], \quad -\pi \le \varphi_n < \pi. \tag{18}$$

The property $|a_n/b_n| = 1$ implies that we restrict ourselves to states with current density $j(x) = 0$. This is cogent when one is looking for localized states. The phases φ_n and φ_{n-1} are connected through the matrix M_n which is written in the form

$$M_n = \begin{pmatrix} \frac{1}{\tau}\exp[i(\theta+\alpha\zeta_n)] & -\frac{\rho}{\tau}\exp[-i(\sigma+\alpha\zeta_n)] \\ -\frac{\rho}{\tau}\exp[i(\sigma+\alpha\zeta_n)] & \frac{1}{\tau}\exp[-i(\theta+\alpha\zeta_n)] \end{pmatrix},$$
$$\zeta_n = 1 + \varepsilon_n - \varepsilon_{n-1}. \tag{19}$$

From $\mathbf{A}_n = M_n\mathbf{A}_{n-1}$ one finds

$$\begin{aligned} a_n &= \frac{a_{n-1}}{\tau}\{\exp[i(\theta+\alpha\zeta_n)] - \\ &\qquad \rho\exp[-i(\varphi_{n-1}+\sigma+\alpha\zeta_n)]\}, \\ b_n &= \frac{b_{n-1}}{\tau}\{\exp[-i(\theta+\alpha\zeta_n)] - \\ &\qquad \rho\exp[i(\varphi_{n-1}+\sigma+\alpha\zeta_n)]\}, \end{aligned} \tag{20}$$

$$\begin{aligned} \exp[i\varphi_n] \equiv \frac{a_n}{b_n} &= \exp[i(2\theta+2\alpha\zeta_n+\varphi_{n-1})] \\ &\quad \cdot \frac{1-\rho\exp[-i\Phi_n]}{1-\rho\exp[+i\Phi_n]}, \end{aligned} \tag{21}$$

where

$$\Phi_n = 2\alpha\zeta_n + \theta + \sigma + \varphi_{n-1}. \tag{22}$$

This suggests a recurrence system for Φ_n instead for φ_n. Introducing the number $\Omega = 2(\theta+\alpha)$, one immediately obtains from (21) and (22)

$$\begin{aligned} &\Phi_{n+1} = F(\Phi_n,\rho) + \Omega + 2\alpha(\varepsilon_{n+1} - \varepsilon_n), \\ &F(\Phi,\rho) = \Phi + 2\gamma(\Phi,\rho), \\ &n = 1,2,\ldots, \quad \Phi_n \in [-\pi,\pi), \end{aligned} \tag{23}$$

where

$$\begin{aligned} &\gamma(\Phi,\rho) = \arg(1-\rho\exp[-i\Phi]) \text{ or} \\ &\tan(\gamma) = \frac{\rho\sin(\Phi)}{1-\rho\cos(\Phi)}. \end{aligned} \tag{24}$$

The inverse function of F with $\Psi = F(\Phi,\rho)$ and $\Phi = F^{-1}(\Psi,\rho)$ is simply given as, see Appendix B,

$$F^{-1}(\Psi,\rho) = F(\Psi,-\rho) \equiv \Psi + 2\gamma(\Psi,-\rho). \tag{25}$$

For $\rho^2 < 1$, which we always assume, the derivative is positive, i. e.

$$\frac{\partial F(\Phi,\rho)}{\partial\Phi} \equiv F'(\Phi) = \frac{1-\rho^2}{1-2\rho\cos(\Phi)+\rho^2} > 0, \tag{26}$$

so that $\Phi \to F(\Phi)$ is bijective in the half open interval $\Phi \in [-\pi, \pi)$. The phase γ can be restricted to the open interval $(-\pi/2, \pi/2)$. From (22) the initial phase is given by

$$\Phi_1 = \Omega - \theta + \sigma + 2\alpha\varepsilon_1 + \varphi_0, \quad \exp[i\varphi_0] = \frac{a_0}{b_0}. \tag{27}$$

By iterating (23), one obtains

$$\begin{aligned} &\Phi_n = 2\alpha\varepsilon_n + n\Omega + \Phi_0 + \Psi_{n-1}, \\ &\Psi_{n-1} = 2\sum_{\mu=1}^{n-1}\gamma(\Phi_\mu,\rho). \end{aligned} \tag{28}$$

At the special energies, where $\rho = 0$ and thus $\Psi_{n-1} \equiv 0$, there is the explicit solution

$$\Phi_n^{(0)} = n\Omega + 2\alpha\varepsilon_n + \Phi_0, \quad \Phi_0 = \sigma - \theta + \varphi_0, \tag{29}$$

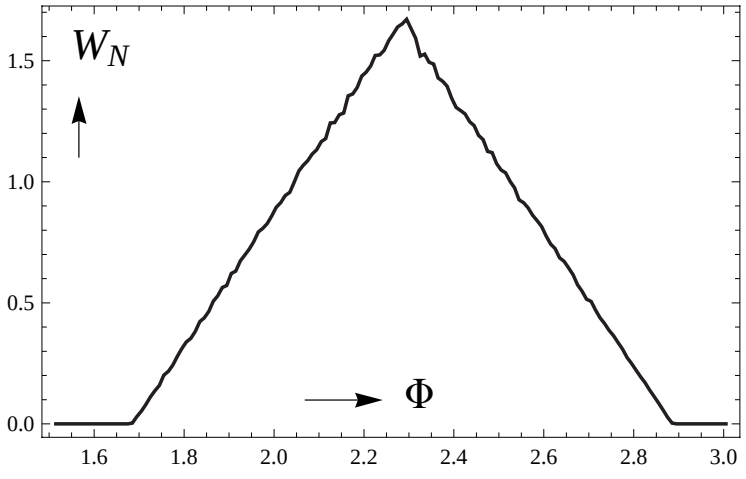

Fig. 1. Computer experimental distribution function $W_N(\Phi)$ of the phases $\{\Phi_1, \Phi_2, \ldots \Phi_N\}$, $N = 10^6$, for a single configuration. The parameter values read: wave number $K = 1$; disorder parameter $\varepsilon^* = 0.1$; bin width $\Delta\Phi = 0.01$; potential strength parameter $K_V = 3.2$; quotient of mean lattice constant by width of scattering potential $d/w = 1.5$. The discrete points are joined by straight lines.

where $\Omega = \lim_{n->\infty} \Phi_n^{(0)}/n$ can be identified as a rotation number [27].

As to the amplitudes A_n, we find from (20) the recurrence relation

$$\begin{aligned} A_n &\equiv \sqrt{|a_n|^2 + |b_n|^2} = x_n A_{n-1}, \\ x_n &= \sqrt{1 + \rho^2 - 2\rho\cos(\Phi_n)}/\tau. \end{aligned} \tag{30}$$

By iteration we obtain $A_n = \prod_{\nu=1}^{n} x_\nu A_0$. Using the relation $\tau = \sqrt{1-\rho^2}$, we arrive at the following expression of the Lyapunov exponent:

$$\Lambda \equiv \overline{\lim}_{N\to\infty} \frac{\ln(A_N)}{N} = \frac{1}{2}\left\{ \overline{\lim}_{N\to\infty} \frac{1}{N} \sum_{n=1}^{N} \ln[1 + \rho^2 - 2\rho\cos(\Phi_n)] - \ln[1-\rho^2] \right\}. \tag{31}$$

Thus, for a given reflection coefficient ρ, the amplitudes A_n and the Lyapunov exponent are fully determined by the phases Φ_n, $n = 1, 2, \ldots$.

As a function of the wave number K, the reflection coefficient ρ can have zeros. For a square barrier potential, there are infinitely many zeros at K_n which are specified in Section 5, equation (56); for illustration see Figure 5. If $\rho = 0$, then the transfer matrices M_n, defined in (19), are unitary. This implies constant amplitudes $A_n = A_0$ for all n, and thus a zero Lyapunov exponent for every disorder configuration of the RDM. Of course, such a behaviour will not be met in the case of random potential strengths when $\rho \to \rho_n$ is different for different sites n.

4. Distribution Function of the Phases Φ_n

We define the distribution function in terms of the periodic Dirac delta function as follows:

$$\begin{aligned} W_N(\Phi) &= \frac{1}{N} \sum_{n=1}^{N} \delta_{\mathrm{per}}(\Phi - \Phi_n), \\ \delta_{\mathrm{per}}(x) &= \sum_{r\in\mathbf{Z}} \delta(x - 2\pi r), \quad \Phi \in [-\pi, \pi). \end{aligned} \tag{32}$$

In Fig. 1 we display the computer experimental distribution function $W_N(\Phi)$ for $K = 1$; the function was integrated over the bin width $\Delta\Phi = 0.01$. In Fig. 1 and henceforth, the wave number and potential parameter K and K_V, respectively, are dimensionless after multiplication with the potential width w. As will be shown in Section 7, the triangular form of the curve can be understood from the analytical asymptotic limit $\rho \to 1$; with the potential parameter $K_V = 3.2$ we have $\rho(K = 1) = 0.9984$. In Fig. 2 the analogous distribution is shown for $K = 4.7$, which corresponds to a much smaller reflectivity with $\rho = 0.0933$. As is seen, $W_N(\Phi) \neq 0$ in the whole interval $\Phi \in [-\pi, \pi)$; the curve corresponds to the analytical approximation (up to order ρ^3) of the functional equation for $W_N(\Phi)$ with $N \to \infty$; see further below.

We assume, that $W(\Phi) = \overline{\lim}_{N\to\infty} W_N(\Phi) = \underline{\lim}_{N\to\infty} W_N(\Phi)$ for almost all disorder configurations $\{\varepsilon_1, \varepsilon_2, \ldots\}$. With $W(\Phi)$, the Lyapunov exponent (31) can be written in the form

$$\begin{aligned} \Lambda &= (\Lambda_1 + \Lambda_2)/2, \\ \Lambda_1 &= \int_{-\pi}^{\pi} \mathrm{d}\Phi\, W(\Phi) \ln[1 - 2\rho\cos(\Phi) + \rho^2], \\ \Lambda_2 &= -\ln(1-\rho^2). \end{aligned} \tag{33}$$

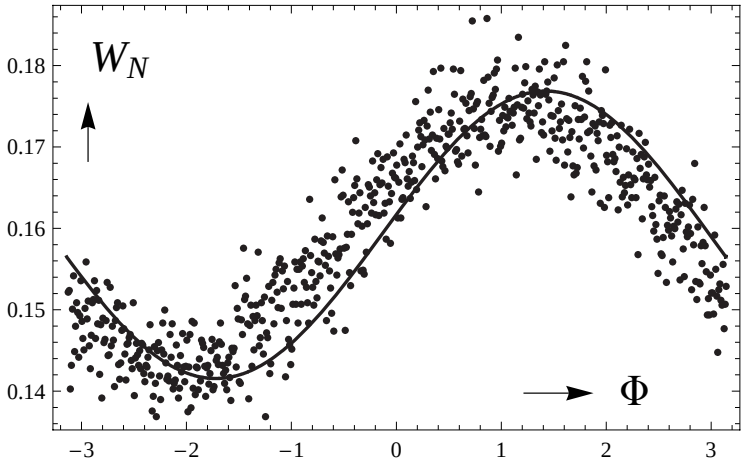

Fig. 2. The same as Fig. 1 for $K = 4.7$ with the same disorder configuration. The by computer experiment obtained point set for $N = 10^6$ is compared with the analytical approximation (up to order ρ^3) of the functional equation for $W(\Phi)$ (solid line), which corresponds to an infinite number of scatterers, $N \to \infty$. As compared to Fig. 1 the plot range of the vertical axis is restricted.

The density $W(\Phi)$ is determined by means of a conditional probability function $V(x)$ for $x \in [-\pi, \pi]$, which obeys the following linear integral equation (see Appendix C, also for interpretation):

$$\begin{aligned} &V(x) = \int_{\mathbf{R}} \mathrm{d}\eta \, p(\eta)[V(Y) - V(Y_0)], \\ &(x, \eta) \to X = x + 2\alpha\eta - \Omega, \\ &X \to Y = F^{-1}(X, \rho), \quad Y_0 = Y(x = -\pi), \end{aligned} \tag{34}$$

where $x \to V = V(x)$ is uniquely determined by the properties

$$V(-\pi) = 0 \text{ and } V(x + 2\pi) = V(x) + 1, \quad x \in \mathbf{R}, \tag{35}$$

which implies that $V(\pi) = 1$, and $V(x) - x/(2\pi)$ is 2π-periodic. The density W is connected to V as follows (see Appendix C):

$$W(\Phi) = \frac{1}{2\alpha} \int_{\mathbf{R}} \mathrm{d}\varepsilon \, p'(\varepsilon) V(\Phi - 2\alpha\varepsilon). \tag{36}$$

As it is easily seen, after partial integration with respect to ε,

$$\int_{-\pi}^{\pi} \mathrm{d}\Phi W(\Phi) = 1. \tag{37}$$

In the case of the special disorder distribution (2), we have

$$p'(\varepsilon) = [\delta(\varepsilon^* + \varepsilon) - \delta(\varepsilon^* - \varepsilon)]/(2\varepsilon^*), \tag{38}$$

which gives rise to

$$W(\Phi) = [V(\Phi + 2\alpha\varepsilon^*) - V(\Phi - 2\alpha\varepsilon^*)]/(4\alpha\varepsilon^*). \tag{39}$$

By means of discretization and for the disorder distribution (2), we have solved the integral equation (34) numerically to high accuracy; e. g. numerical normalization error of $W(\Phi)$, with the aid of the trapezoidal rule, was of the order 10^{-15}. The computer code is outlined in Appendix A. Basically, this code serves to examine empirically in which wave number intervals our analytical approaches are acceptable approximations. For our standard model (see caption of Fig. 1, but variable K), the asymptotic formulas for $\rho \to 1$ are quantatively reliable in the interval $0 \le K < 2$. In the opposite limit, $\rho \to 0$, the asymptotic formula given in (55) and numerical evaluation of the integral equation are in good agreement for $K > 6$, see Figs. 3 and 4.

In principle, results can also be obtained by direct numerical simulation of the recurrence system (23) which was applied to obtain Fig. 1 and the point set of Figure 2. However, for a given number N of scatterers, the fluctuations increase with wave number (or equivalently with decreasing reflection coefficient ρ). One can see this, e. g., by comparing Fig. 2 ($\rho = 0.0933$) with Fig. 1 ($\rho = 0.9984$). Going to smaller ρ, the number N, which is required to obtain results above the noise level, soon becomes prohibitively large. The integral equation (34), on the other hand, implies the limit $N \to \infty$.

5. Perturbation Theory for Small Reflection Coefficient

In order to solve the integral equation perturbatively up to third order in ρ, we make the ansatz

$$V(x) = V_0(x) + \rho V_1(x) + \rho^2 V_2(x) + \rho^3 V_3(x), \tag{40}$$

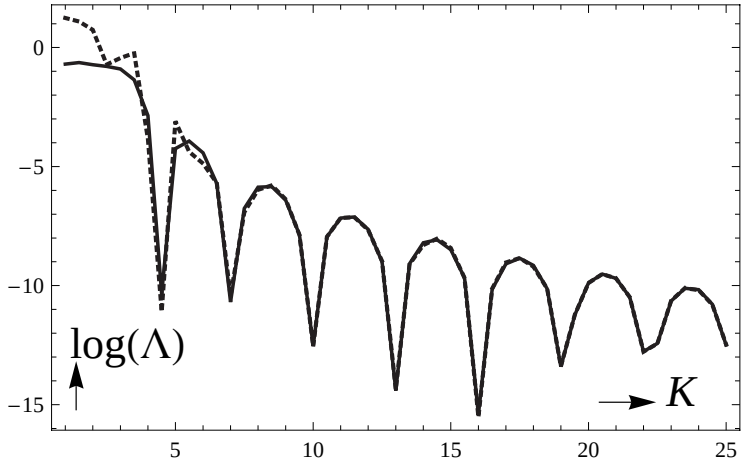

Fig. 3. Natural logarithm of Lyapunov exponent Λ as a function of the wave number K calculated at $K \to K^{(j)} = 1 + 1/2\,j$, $j = 0, 1, \ldots, 48$. The discrete points $\Lambda(K^{(j)})$ are joined by straight dashed and solid lines for the numerical solution of integral equation (34) and the analytical expression $\Lambda^{(2)}$ as given in (55), respectively. The two curves practically coincide for $K > 6$. There is an almost coincidence of the discrete point $K^{(30)} = 16$ and the fifth zero of $\rho(K_n) = 0$ at $K_5 = 16.0306$ [see (56)], where the Lyapunov exponent is exactly zero.

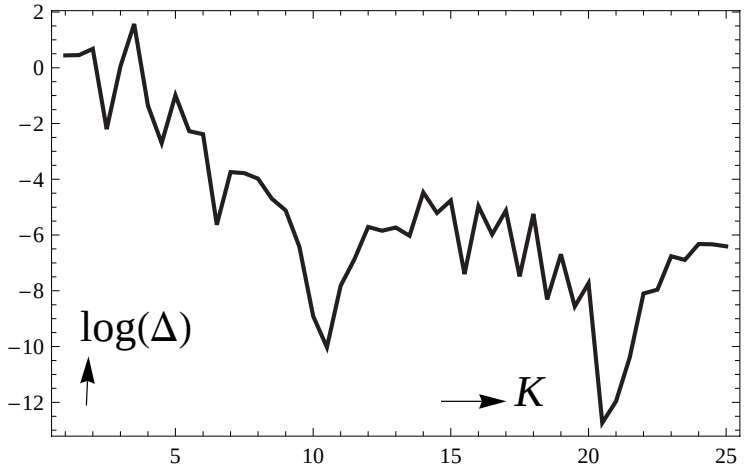

Fig. 4. Natural logarithm of relative error $\Delta = |\log(\Lambda) - \log(\Lambda^{(2)})|/|\log(\Lambda)|$ as a function of the wave number K calculated at $K \to K^{(j)} = 1 + 1/2\,j$, $j = 0, 1, \ldots, 48$ corresponding to Figure 3. The discrete points $\log(\Delta(K^{(j)}))$ are joined by straight lines.

and use the series representation (see Appendix B)

$$F(\Phi,\rho) = \Phi + 2\sum_{r=1,2,\ldots} \rho^r \frac{\sin(r\Phi)}{r}, \qquad F^{-1}(\Phi,\rho) = F(\Phi,-\rho). \tag{41}$$

For simplicity, we assume symmetric disorder distributions, $p(\varepsilon) = p(-\varepsilon)$. With the notation of the Fourier transform

$$p_n = \int_{\mathbf{R}} \mathrm{d}\varepsilon\, p(\varepsilon)\exp(-2in\alpha\varepsilon) = \int_{\mathbf{R}} \mathrm{d}\varepsilon\, p(\varepsilon)\cos(2n\alpha\varepsilon) \tag{42}$$

and the abbreviations

$$D_n = 1 - 2p_n\cos(n\Omega) + (p_n)^2, \quad n = 1, 2, \ldots, \tag{43}$$

the formal series expansion of (34) leads to the following recurrence structure:

$$V_n(x) - \int_{\mathbf{R}} \mathrm{d}\eta\, p(\eta) V_n(X) = \int_{\mathbf{R}} \mathrm{d}\eta\, p(\eta)[G_{n-1}(Y) - G_{n-1}(Y_0) - V_n(Y_0)], \tag{44}$$

where the function G_{n-1} is known in terms of the lower-order functions $V_0, \ldots V_{n-1}$. The dependence on ρ enters explicitely through the ansatz (40), and implicitely through the argument Y: $V(Y) \equiv V(F^{-1}(X,\rho))$. To zero order in ρ, we can replace in (34) $Y = F^{-1}(X,\rho)$ by $Y = X \equiv x + 2\alpha\eta - \Omega$, and obtain the unique solution $V_0(x) = (x+\pi)/(2\pi)$, which obeys the conditions (35). As a consequence, the functions $V_1(x), V_2(x), \ldots$ are periodic with $V_n(-\pi) =$

0. We insert the following ansatz into (44):

$$V_n(x) = \sum_{\nu\in\mathbf{Z}} c_\nu^{(n)} \exp[i\nu x], \quad n = 1,2,\ldots, \tag{45}$$

and compare the coefficients of the independent functions $\exp[\mathrm{i}mx]$, $m \in \mathbf{Z}$, which lead to the equations

$$c_m^{(n)}[1 - p_m \exp(-\mathrm{i}m\Omega)] = \int_{\mathbf{R}} \mathrm{d}\eta\, p(\eta)[G_{n-1}(Y)]_m \tag{46}$$

and

$$\int_{\mathbf{R}} \mathrm{d}\eta\, p(\eta)[G_{n-1}(Y_0) + V_n(Y_0)] = 0, \tag{47}$$

where $[..]_m$ denotes the coefficient of $\exp[\mathrm{i}mx]$. By the definition (42), $p_0 = 1$. We assume that $|p_m| < 1$ if $m \neq 0$, to be discussed later. Then, the coefficients $c_m^{(n)}$ are determined through (46) except for $c_0^{(n)}$, which is needed to fulfill (47); the $m = 0$ component $[G_{n-1}(Y)]_{m\to 0}$ can be set equal to zero. The algebraic manipulations required were carried out by means of Mathematica [28]. Below, we write the solution with $V_3(x)$ in a less explicit form to avoid clumsy expressions:

$$V_0(x) = (x+\pi)/(2\pi), \tag{48}$$

$$V_1(x) = \frac{p_1}{\pi D_1}[\sin(\Omega) + \sin(\Omega - x) + p_1 \sin(x)], \tag{49}$$

$$\begin{aligned} V_2(x) = \frac{p_2}{2\pi D_1 D_2}\{&p_1(1+p_2)[\sin(\Omega - 2x) - \sin(\Omega)] \\ &+ p_1 p_2[\sin(\Omega + 2x) - \sin(\Omega)] \\ &+ ((p_1)^2 - 1)[\sin(2\Omega - 2x) - \sin(2\Omega)] \\ &- p_1[\sin(3\Omega - 2x) - \sin(3\Omega)] \\ &+ p_2((p_1)^2 - 1)\sin(2x)\}, \end{aligned} \tag{50}$$

$$\begin{aligned} V_3(x) &= c_0^{(3)} + \{c_1^{(3)} \exp(\mathrm{i}x) + c_3^{(3)} \exp(3\mathrm{i}x) + c.c.\}, \\ c_1^{(3)} &= \frac{\mathrm{i}p_1}{2\pi (D_1)^2 D_2}[p_1 - \exp(-\mathrm{i}\Omega)]^2 \\ &\quad \cdot [p_1 + p_2 \exp(-\mathrm{i}\Omega)][p_2 \exp(2\mathrm{i}\Omega) - 1], \\ c_3^{(3)} &= \frac{\mathrm{i}p_3}{6\pi D_1 D_2 D_3}[\exp(-\mathrm{i}\Omega) - p_1][p_2 - \exp(-2\mathrm{i}\Omega)] \\ &\quad \cdot \{\exp(3\mathrm{i}\Omega) + 2p_1 \exp(2\mathrm{i}\Omega) + 2p_2 \exp(\mathrm{i}\Omega) \\ &\quad + p_1 p_2\}[p_3 - \exp(-3\mathrm{i}\Omega)], \\ c_0^{(3)} &= -\int \mathrm{d}\eta\, p(\eta) G_2(Y_0) + \{p_1 c_1^{(3)} \exp(-\mathrm{i}\Omega) \\ &\quad + p_3 c_3^{(3)} \exp(-3\mathrm{i}\Omega) + c.c.\}, \end{aligned}$$

$$\begin{aligned} G_2(Y_0) = &-\frac{2}{6\pi}\sin(3Y_0) + \sin(2Y_0)V_1'(Y_0) \\ &- 2\sin(Y_0)V_2'(Y_0) + 2\sin^2(Y_0)V_1''(Y_0), \\ Y_0 = &-\pi - \Omega + 2\alpha\eta. \end{aligned} \tag{51}$$

For the ansatz (40), the conditions (36) are fulfilled.

Let us apply the approximation to the Λ_1 term of the Lyapunov exponent, given in (33). To this end we make use of the Fourier representation (see Appendix B)

$$\ln[1 - 2\rho\cos(\Phi) + \rho^2] = -2\sum_{s=1,2,\ldots} \rho^s \frac{\cos(s\Phi)}{s}. \tag{52}$$

With reference to (36), we first integrate with respect to Φ:

$$\begin{aligned} \Lambda_1 = \frac{1}{2\alpha}\int_{\mathbf{R}} \mathrm{d}\varepsilon\, p'(\varepsilon) \int_{-\pi}^{\pi} \mathrm{d}\Phi\, \ln[1 - 2\rho\cos(\Phi) + \rho^2] \\ \cdot V(\Phi - 2\alpha\varepsilon). \end{aligned} \tag{53}$$

The Φ integral is carried out up to order ρ^4, but we omit to write down here the rather awkward fourth-order term. With the aid of partial integration we obtain

$$\begin{aligned} \Lambda_1 &= \frac{p_1}{\alpha D_1}\int_{\mathbf{R}} \mathrm{d}\varepsilon p'(\varepsilon)[p_1 \sin(2\alpha\varepsilon) - \sin(\Omega + 2\alpha\varepsilon)]\rho^2 \\ &\quad + \mathcal{O}(\rho^4) \\ &= \frac{2(p_1)^2}{D_1}[\cos(\Omega) - p_1]\rho^2 + \mathcal{O}(\rho^4). \end{aligned} \tag{54}$$

First- and third-order terms are exactly zero. We now add from (33) the term $\Lambda_2 = \rho^2 + \mathcal{O}(\rho^4)$ and take into account the factor 1/2 to arrive at

$$\begin{aligned} \Lambda &= \Lambda^{(2)} + \mathcal{O}(\rho^4), \\ \Lambda^{(2)} &= \frac{\rho^2}{2}\frac{1 - p_1}{1 + (p_1)^2 - 2p_1\cos(\Omega)} \\ &\quad \cdot \{1 + p_1 + 2(p_1)^2 - 2p_1\cos(\Omega)\}. \end{aligned} \tag{55}$$

As it is immediately seen, the regular case, with $p(\varepsilon) = \delta(\varepsilon)$, implying $p_1 = 1$, is correctly reached to second order with $\Lambda^{(2)} = 0$. The same is true to fourth order, which is not shown here. We remark that the limit to the regular case is somewhat delicate. Depending on ρ one has to exclude a measure zero set of rotation numbers Ω before going to the limit. If $\rho = 0$, this can be directly seen from the special case (29) which leads to qualitatively different distributions $W(\Phi)$ for rational and irrational Ω, respectively.

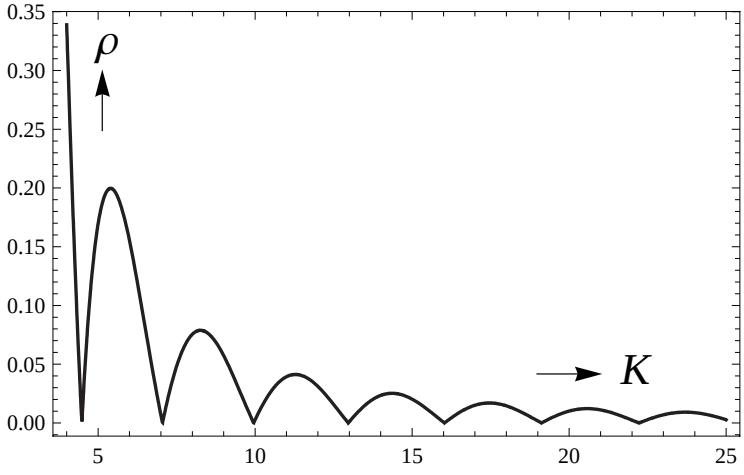

Fig. 5. Reflection coefficient ρ as a function of the wave number K for a square barrier potential.

In Fig. 3, we compare the asymptotic approximation $\Lambda^{(2)}$ with the numerical solution of the integral equation, which in principle should give the true value of Λ. The corresponding relative error is plotted in Figure 4. As it is seen, the relative error lies below 2% for $K > 6$. In Fig. 5, we display the reflection coefficient ρ as a function of K, which explains the oscillating behaviour of Λ and $\Lambda^{(2)}$. As mentioned in Section 3, the Lyapunov exponent is exactly zero at wave numbers K_n, where the reflection coefficient ρ is zero. In the given case of a square barrier potential, the zeros are given by

$$(K_n)^2 = (K_V)^2 + \pi^2 n^2, \quad n \in \mathbf{N}. \tag{56}$$

6. Is the Asymptotic Lyapunov Exponent Positive?

According to mathematical theorems on the random displacement model [22], the function $\Lambda^{(2)}$ should be positive in order that the self-adjoined problem (physical boundary conditions) implies exponentially decaying eigenstates, almost always. Surprisingly to the author, $\Lambda^{(2)}$ is not positive definite when considered as a function of the independent variables $p_1 \in (-1,1)$ and $\Omega \in [-\pi,\pi)$. Before we show this, let us discuss the assumption $|p_n| < 1$, $n = 1,2,\ldots$, which in view of (46) ensures a well defined formal series expansion of the integral equation (34).

As a matter of fact, the condition $|p_n| < 1$ is true for a large class of symmetric disorder distributions $p(\varepsilon)$. To see this, we estimate p_n for $n = 1,2,\ldots$, in the spirit of the mean value theorem of integrals, by choosing the minimum and maximum value of $\cos(y\varepsilon)$, respectively. Since $\int p(\varepsilon) = 1$, we get simply

$$-1 \le \hat{p}(y) \equiv \int \mathrm{d}\varepsilon\, p(\varepsilon)\cos(y\varepsilon) \le 1. \tag{57}$$

Clearly, $\hat{p}(0) = 1$. However, if $y \neq 0$ and p is reasonably smooth, then $\cos(y\varepsilon)$ cannot stick to its maximal or minimal value ± 1 in the whole integration interval. For the piecewise constant distribution (2) we have

$$\hat{p}(y) = \sin(y)/y, \quad p_1 = \hat{p}(2\alpha\varepsilon^*) \tag{58}$$

with $|\sin(y)| < |y|$ for $y \neq 0$. In the case of asymmetric $p(\varepsilon)$, we have still the property $|\hat{p}(y)| \le 1$, because $|\int p(\varepsilon)\exp(\mathrm{i}y\varepsilon)| \le \int p(\varepsilon) = 1$. However, for $y \neq 0$ the mean value argument does not work any more. In any case, for large wave numbers K, the argument $\alpha = dK$ is large, and if the function $p(\varepsilon)$ is sufficiently smooth, then $p_1 = p_1(2\alpha\varepsilon^*)$ decays with some power $1/K^n$, which asymptotically guarantees $|p_n| < 1$ also for asymmetric disorder distributions.

As a counter example, the Bernoulli distribution $p(\varepsilon) = 1/2\,[\delta(\varepsilon+\varepsilon^*) + \delta(\varepsilon-\varepsilon^*)]$ with Fourier transform $\cos(y\varepsilon^*) \equiv \cos(2n\alpha\varepsilon^*)$ leads to $|p_n| = 1$ at discrete values of K, and could cause zero or small denominators in (46). In the existence proofs for the random displacement model [22], some continuity of $p(\varepsilon)$ was adopted which excludes discrete distributions.

Let us discuss the sign of $\Lambda^{(2)}$ which is determined by the factor $L = 1 + p_1 + 2(p_1)^2 - 2p_1\cos(\Omega)$ in (55). If p_1 is positive, then L is minimal when $\cos(\Omega) = 1$ with

$$L \ge 1 - p_1 + 2(p_1)^2 \ge 1 - p_1 > 0, \quad 0 \le p_1 < 1. \tag{59}$$

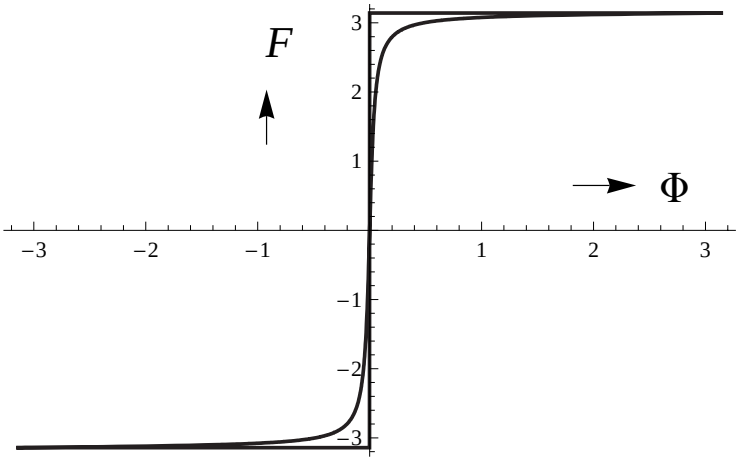

Fig. 6. Comparison between the map $\Phi \to F(\Phi)$ (smooth curve) and its approximation $F_{\rm app}$ for $K = 2.5$ with $\rho = 0.9655$.

On the other hand, for negative p_1 we set $\cos(\Omega) = -1$ with the consequence

$$L \geq L_{\min} = 1 + 3p_1 + 2(p_1)^2, \quad -1 < p_1 < 0. \quad (60)$$

The function $L(p_1, \Omega = -\pi) \equiv L_{\min}$ has zeros at $p_1 = -1$ and $p_1 = -1/2$, and is negative in between with $L_{\min} < 0$, if $(-1) < p_1 < -1/2$. This means that there is the possibility of negative Lyapunov exponents in an interval of nonzero measure. We cannot assume $\cos(\Omega)$ being sufficiently above the value (-1), because the rotation number $\Omega = 2(\theta + \alpha)$, essentially, varies linearly with K; the delay phase θ of a single barrier potential is negative and approaches zero for large wave numbers.

Therefore, in order to have positive Lyapunov exponents asymptotically, which is in agreement with mathematical existence theorems, we are forced to demand the condition $p_1 > -1/2$.

This property is fulfilled for the distribution (2) with Fourier transform $\hat{p}(y) > -0.21723$. We have checked other symmetric functions with increasing higher continuity of the form

$$p^{(n)}(\varepsilon) = b_n[(\varepsilon^*)^2 - \varepsilon^2]^n \Theta(\varepsilon^* - |\varepsilon|), \; n = 1, 2, \ldots. \quad (61)$$

With the normalization constants $b_1 = 3/4\,(\varepsilon^*)^{-3}$, $b_2 = 15/16\,(\varepsilon^*)^{-5}$, $b_3 = 35/32(\varepsilon^*)^{-7}$, we found increasing lower bounds of the corresponding Fourier transforms: $\hat{p}^{(1)}(y) > -0.086$, $\hat{p}^{(2)}(y) > -0.041$, $\hat{p}^{(3)}(y) > -0.0215$. So, one may guess the existence of the following theorem: Given a symmetric distribution function $p(\varepsilon) \geq 0$ of finite support, and normalized to 1, then its Fourier transform is larger $-1/2$ provided the first or higher derivatives of $p(\varepsilon)$ are integrable.

We see no conflict with Theorem 1.2 of [22], where Anderson localization was proved for the given model under the following conditions on the disorder distribution $p(\varepsilon)$: (1) finite support in order to ensure nonoverlapping scattering potentials; (2) continuity (more precisely "nontrivial absolutely continuous component"); (3) $p(\varepsilon) \geq 0$ by definition as a probability density. These restrictions on $p(\varepsilon)$ necessarily do not allow for arbitrary Fourier transforms $\hat{p}(y)$.

7. Approximation of $W(\Phi)$ for ρ Close to 1

In this section we infer an analytical approximation of the distribution function $W(\Phi)$ directly from the recurrence system (23). The map F in the recurrence system (23) is approximated by the step function $F_{\rm app}$:

$$F_{\rm app}(\Phi) = \mathrm{sign}(\Phi)\,\pi, \quad \Phi \in [-\pi, \pi). \quad (62)$$

As will be derived further below, from the map $F_{\rm app}$ and the disorder distribution (2) one obtains the probability density in the form

$$W_{\rm app}(\Phi) = \frac{1}{4\alpha\varepsilon^*} \sum_{r \in \mathbf{Z}} f_r(\Phi),$$
$$f_r = (1 - |z_r|)\Theta(1 - |z_r|), \quad z_r = \frac{\Phi - \Omega_r}{4\alpha\varepsilon^*} \quad (63)$$

with $\Omega_r = -\pi + \Omega + 2\pi r$. In Figs. 6 and 7 we exemplarily compare $F_{\rm app}$ with F, and $W_{\rm app}(\Phi)$ with $W(\Phi)$ and $W_N(\Phi)$, respectively, where the latter was experimentally produced by computer for a single disorder configuration with $N = 10^6$. The parameter chosen, $K = 2.5$ (which implies $\rho = 0.965521$), is already too large for a good quantitative correspondence; but in the

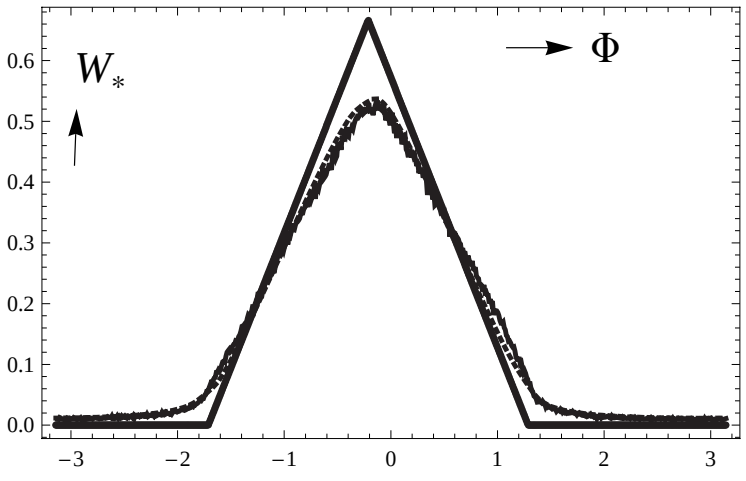

Fig. 7. Comparison of three methods corresponding to Fig. 6 with $K = 2.5$: direct simulation of $W_* \equiv W_N(\Phi)$ as in Fig. 1 with $N = 10^6$; analytical approximation by $W_* \equiv W_{\rm app}(\Phi)$ (triangle curve); numerical solution of the functional equation for $W_* \equiv W(\Phi)$, supposed to give the "true" curve in the limit $N \to \infty$ (dashed curve). The latter coincides closely with the empirical curve.

interval $0 \le K \le 2.0$ the three curves coincide graphically.

In order to prove (63), it is first observed that the phases Φ_n of the recursion (23) are taken modulo 2π. Thus, the function $F_{\rm app}$ simply maps the half-open interval $\Phi \in [-\pi, \pi)$ into the constant $-\pi$:

$$F_{\rm app}(\Phi) = -\pi \ \text{ modulo } \ 2\pi, \quad -\pi \le \Phi < \pi. \tag{64}$$

The probability density for Φ follows from the definition (32) of $W_N(\Phi)$, from the recursion (23) with $\Phi_n = -\pi + \Omega + 2\alpha(\varepsilon_n - \varepsilon_{n-1})$, and the configuration average in the limit $N \to \infty$:

$$\begin{aligned} &W_{\rm app}(\Phi) = \\ &\sum_{r\in\mathbf{Z}} \int {\rm d}\varepsilon {\rm d}\varepsilon'\, p(\varepsilon) p(\varepsilon')\, \delta(\Phi - \Omega_r - 2\alpha(\varepsilon' - \varepsilon)), \\ &\Omega_r = -\pi + \Omega + 2\pi r. \end{aligned} \tag{65}$$

The normalization is fulfilled:

$$\int_{-\pi}^{\pi} {\rm d}\Phi\, W_{\rm app}(\Phi) = 1. \tag{66}$$

For the disorder distribution (2), integration with respect to ε' leads to

$$\begin{aligned} W_{\rm app}(\Phi) &= \frac{1}{8\alpha(\varepsilon^*)^2} \sum_{r\in\mathbf{Z}} \int {\rm d}\varepsilon\, \Theta(\varepsilon^* - |\varepsilon|) \\ &\qquad \cdot \Theta(\varepsilon^* - |\varepsilon + 2\varepsilon^* z_r|) \\ &= \frac{1}{8\alpha\varepsilon^*} \sum_{r\in\mathbf{Z}} \int_{-1}^{1} {\rm d}y\, \Theta(1 - |y|) \\ &\qquad \cdot \Theta(1 - |y + 2z_r|), \\ y &= \varepsilon/\varepsilon^*. \end{aligned} \tag{67}$$

The integral in (67) has the symmetry $z_r \to -z_r$ and is zero, if $|z_r| > 1$. On the other hand, if $|z_r| < 1$, the integral is equal to the length Δ of the overlap interval of the the two Θ functions in (67). This interval is linear in $|z_r|$, and from the extreme cases $\Delta(|z_r| = 0) = 2$ and $\Delta(|z_r| = 1) = 0$ one immediately finds $\Delta = 2(1 - |z_r|)$. Thus, we end up with the result (63).

How does $W_{\rm app}$ look like as a function of Φ? It is obviously continuous, and it is not hard to prove that it has exactly one peak maximum at Φ_p and two kinks at $\Phi_\pm$. The three points form a triangle (modulo 2π) which is superimposed over a constant level W_0, which is zero for low K values. We remind that Φ and Ω are reduced to the half-open interval $[-\pi, \pi)$. There are unique integers r_0, r_1, r_2 with $z_{r_0} = 0$, which determines the peak, and the conditions $z_{r_1} = 1$, $z_{r_2} = -1$ give the locations of the two kinks:

$$\begin{aligned} \Phi_p &= \Omega_{r_0} \ \text{ modulo } \ 2\pi, \\ \Phi_+ &= +4\alpha\varepsilon^* + \Omega_{r_1} \ \text{ modulo } \ 2\pi, \\ \Phi_- &= -4\alpha\varepsilon^* + \Omega_{r_2} \ \text{ modulo } \ 2\pi. \end{aligned} \tag{68}$$

For example, for $K = 1$ we have $\Omega = -0.86592$ which leads to $\Phi_p = 2.27567$, $\Phi_+ = 2.87567$, and $\Phi_- = 1.67567$ corresponding to the integers $r_0 = r_1 = r_2 = 1$. The corresponding $W_{\rm app}$ reproduces the empirical distribution of Fig. 1 within about 1% relative deviations.

By continuity of $W_{\rm app}(\Phi)$, the constant level W_0 is given by $W_0 = W_{\rm app}(\Phi_+) = W_{\rm app}(\Phi_-)$. In order that $W_0 > 0$, there must exist at least one integer $r \ne r_1$ or $r \ne r_2$ such that

$$\begin{aligned} &|z_r(\Phi_+)| < 1, \quad r \ne r_1, \ \text{ or} \\ &|z_r(\Phi_-)| < 1, \quad r \ne r_2. \end{aligned} \tag{69}$$

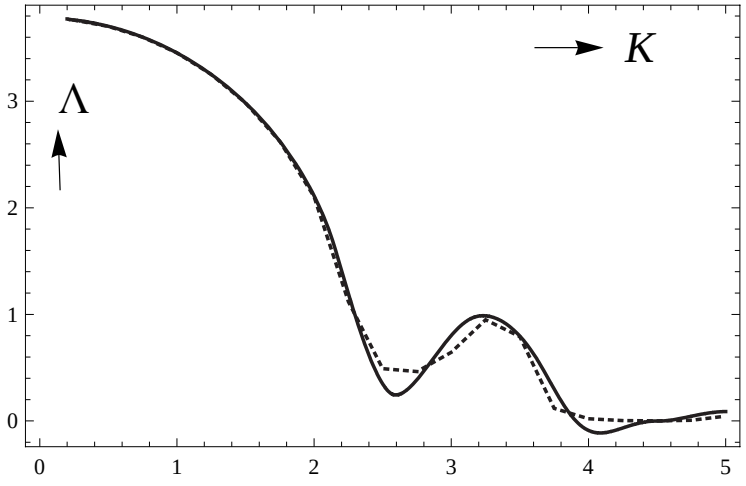

Fig. 8. Lyapunov exponent Λ as a function of the wave number K. Comparison of the analytical expression $\Lambda_{\rm app}$ (solid line) and the numerical solution of the functional equation for $W(\Phi)$. The analytical result should be asymptotically exact in the limit $K \to 0$ (reflection coefficient $\rho \to 1$). The dashed curve, supposed to give the "true" value, was calculated at the discrete points $K_i = i/4$, $i = 1,\ldots,20$; the points were joined by straight dashed lines.

This amounts to the condition, that a natural number n must exist with the property

$$2\pi n < 8\alpha\varepsilon^* \quad \text{for at least one} \quad n \in \{1,2,\ldots\}. \tag{70}$$

With $\varepsilon^* = 0.1$, $d/w = 1.5$, $\alpha \equiv dK$ we find that $wK > \pi/0.6 \approx 5.236$ gives rise to $W_0 > 0$. In other words, in the interval $0 \le K \le 2$, where $W_{\rm app}$ is a good quantitative approximation with the disorder distribution (2), the level $W_0 = 0$.

The Lyapunov exponent related to $W_{\rm app}(\Phi)$ can be given in the following closed form:

$$\Lambda_{\rm app} = -\sum_{s=1,2,\ldots} \frac{(-\rho)^s}{s^3} \frac{\sin^2(2\alpha\varepsilon^* s)}{8\alpha^2(\varepsilon^*)^2} \cos(s\Omega) - \frac{1}{2}\ln[1-\rho^2]. \tag{71}$$

To prove (71), we will first restrict to sufficiently low K values which implies that $W_0 = 0$. Furthermore, the integers in (68), $r_0 = r_1 = r_2 = 1$, lead to

$$\begin{aligned} &\Phi_p = \pi + \Omega, \quad \Phi_- = -4\alpha\varepsilon^* + \pi + \Omega, \\ &\Phi_+ = 4\alpha\varepsilon^* + \pi + \Omega, \quad W(\Phi_p) = 1/(4\alpha\varepsilon^*), \\ &W(\Phi_-) = 0, \quad W(\Phi_+) = 0. \end{aligned} \tag{72}$$

The result for low K will continuously extend to arbitary $K > 0$. In view of (33) and (52), the integral to be carried out reads

$$\begin{aligned} \Lambda_1^{\rm app} &= \int_{-\pi}^{\pi} {\rm d}\Phi\, W_{\rm app}(\Phi) \ln[1+\rho^2-2\rho\cos(\Phi)] \\ &= -2\sum_{s=1,2,\ldots} \frac{\rho^s}{s} L_s, \\ L_s &= \int_{-\pi}^{\pi} {\rm d}\Phi\, W_{\rm app} \cos(s\Phi). \end{aligned} \tag{73}$$

For low K, the distribution $W_{\rm app}(\Phi)$ is of triangular form and of the type shown in Figure 1. There are two contributions from the intervals $\Phi_- \le \Phi \le \Phi_p$ and $\Phi_p \le \Phi \le \Phi_+$, where $W_{\rm app}$ is linear in Φ:

$$L_s = \frac{1}{16\alpha^2(\varepsilon^*)^2} \left\{ \int_{\Phi_-}^{\Phi_p} {\rm d}\Phi\,(\Phi - \Phi_-) + \int_{\Phi_p}^{\Phi_+} {\rm d}\Phi\,(-\Phi + \Phi_+) \right\} \cos(s\Phi). \tag{74}$$

Evaluation of the integral leads to

$$L_s = (-1)^s \frac{\sin^2(2\alpha\varepsilon^* s)}{8\alpha^2(\varepsilon^*)^2 s^2} \cos(s\Omega), \tag{75}$$

which in view of (33) gives the result (71). In Fig. 8 we display $\Lambda_{\rm app}$ in the interval $0.2 \le wK \le 5$, in comparison with the numerical solution of the integral equation (34) in connection with (39). As it is seen, there is the expected agreement for low K values, specifically for $K < 2$.

8. Conclusions

The Lyapunov exponent was determined by three independent methods: (1) the direct simulation of the relevant transfer matrix phases; (2) the numerical solution of a functional equation for the distribution of the phases; (3) analytical asymptotic formulas for the distribution function. Method (1) was feasible up to about 10^6 scatterers and delivered useful results in the low wave number range (high reflectivity), for approximately $K < 5$. With increasing wave number the noise level made it more and more difficult to infer a distribution function by means of computer simulation.

Method (2) turned out to be the most versatile. A cumulative distribution, i. e. a monotonically increasing function, had to be calculated from a linear integral equation; the computer code turned out to be particularly stable and accurate. With the aid of this code, the asymptotic analytical distributions were corroborated with the result that the low wave number asymptotics is quantitavely reliable for $0 \leq K < 2$, and the high wave number asymptotics for $K > 6$. In the latter case, surprisingly, the Lyapunov exponent could be negative, in principle. It was always positive, if the Fourier tranform of the disorder distribution $p(\varepsilon)$ was bounded from below in the following way: if $p(\varepsilon) = p(-\varepsilon)$ is symmetric, then $\hat{p}(y) = \int p(\varepsilon)\cos(y\varepsilon)$ has to obey $\hat{p} > -1/2$. We examined several distributions of finite support and of different degree of continuity which all fulfilled this condition. We did not see a contradiction to the main theorem of [22], where the assumptions on the disorder distribution function are formulated in direct rather than in Fourier space.

Appendix

A. Computer Code for the Integral Equation (34)

We briefly outline the computer code to solve the integral equation (34). This is done by means of a Mathematica "module" [28]. The basic interval $x \in [-\pi, \pi]$ is divided into N equal subintervals with abscissas $x_i = -\pi + 2\pi(i-1)/N$, $i = 1,2,\ldots N+1$. The unknown function values $V_i \equiv V(x_i)$ are labelled as $V_i \to z^i$, where z is a generating variable. For each x_i, one determines $x_i \to X_i = x_i - \Omega + 2\alpha\eta$, $X_i \to Y = F^{-1}(X_i, \rho)$. The parameter Ω is defined below (22), and easily determined, modulo 2π, for a square barrier potential; for explicit expressions of the latter see for e. g. [29]. By the relation (25) one calculates the inverse function as $F^{-1}(X_i,\rho) = X_i + 2\arg[1 + \rho\exp(-\mathrm{i}X_i)]$. In order to integrate with respect to η, one divides the integration interval $\eta \in [-\varepsilon^*, \varepsilon^*]$ into M equal subintervals with abscissas $\eta_1, \ldots \eta_{M+1}$. Integration is done with the trapezoidal rule. Not all points $Y_{ij} \equiv Y(x_i, \eta_j)$ lie in the basic interval. Before reduction it is wise to identify the smallest and largest abscissa, whose function values have to be multiplied by the factor 1/2 in the trapezoidal rule, while the remaining values get the weight one and are on equal footing. If the reduced value of Y_{ij} falls into the interval $[x_n, x_{n+1})$, then the function value is linearly interpolated so that $Y_{ij} \to V(Y_{ij}) \equiv a_{ij}z^n + b_{ij}z^{n+1} + n_{ij}$, where n_{ij} is an integer determined by the condition $V(Y_{ij} + 2\pi) = V(Y_{ij}) + 1$. Example: If $Y_{ij} = -2\pi$, then we have to add 2π for reduction into the basic interval $(-\pi, \pi)$, and thus $V(Y_{ij}) \equiv V(Y_{ij} + 2\pi - 2\pi) = V(Y_{ij} + 2\pi) - 1$. The integral equation (34) is thus replaced by $(N+1)$ linear equations $V(x_i) = L_i(V(x_1), \ldots, V(x_{N+1}))$, $i = 1,2,\ldots N+1$. The first equation is identically fulfilled because on the left-hand side of (34) $V(x_1) \equiv V(-\pi) = 0$, and on the right-hand side $Y(x_1) \equiv Y_0$. In the last equation, because of (35), $V(x_{N+1}) = V(\pi) = 1$, whereas on the right-hand side of (34) $Y(x_{N+1}, \eta_j) \equiv Y(\pi, \eta_j) = Y_0(\eta_j) + 2\pi$; thus $V(Y(\pi,\eta_j)) - V(Y_0(\eta_j)) = V(Y_0) + 1 - V(Y_0) = 1$. As a consequence, the first and last equation are identically fulfilled, and we stay with $(N-1)$ equations for the $(N-1)$ powers $V(x_i) \longleftrightarrow z^i$, $i = 2,3,\ldots,N$. In the equations one has to replace $z \leftrightarrow V(-\pi)$ by zero, and $z^{N+1} \leftrightarrow V(\pi)$ by the number 1. The coefficient matrix of the powers $z^2, \ldots, z^N$ is extracted by the Mathematica command "Coefficient[..]". One run, with $N = 200$ and $M = 123$, on a modern notebook takes about 10 s.

B. Proofs of Formulas Used

In the following we state and prove formulas which were used in the main text and are required in the next appendices. Most statements refer to the map F:

$$F(\Phi,\rho) = \Phi + 2\gamma(\Phi,\rho),$$
$$\tan(\gamma) = \frac{\rho\sin(\Phi)}{1-\rho\cos(\Phi)}. \tag{B.1}$$

(I)
$$\frac{\partial F(x,\rho)}{\partial x} \equiv F'(x,\rho) = \frac{1-\rho^2}{1+\rho^2-2\rho\cos(x)},\ \rho^2 < 1. \tag{B.2}$$

(II)
$$F^{-1}(x,\rho) = F(x,-\rho) \text{ or } F(F(x,-\rho),\rho) = F(F(x,\rho),-\rho) \equiv x. \tag{B.3}$$

(III)
$$\frac{\partial F(z,\rho)}{\partial z} \equiv F'(z,\rho) = \frac{1+\rho^2+2\rho\cos(x)}{1-\rho^2}, \quad x = F(z,\rho). \tag{B.4}$$

(IV)
$$\exp[\mathrm{i}z] = \frac{\rho + \exp[\mathrm{i}x]}{1+\rho\exp[\mathrm{i}x]}, \quad x = F(z,\rho).$$

(IVa)
$$\cos(z) = \frac{2\rho + \cos(x) + \rho^2\cos(x)}{1+\rho^2+2\rho\cos(x)}. \tag{B.5}$$

(IVb)
$$\sin(z) = \frac{(1-\rho^2)\sin(x)}{1+\rho^2+2\rho\cos(x)}.$$

(V) $F(x,\rho)$

$$\equiv x+2\gamma(x,\rho)=x+2\sum_{n=1,2,\ldots}\rho^n\frac{\sin(nx)}{n}, \quad \rho^2<1. \tag{B.6}$$

(VI) $\ln(1-2\rho\cos(x)+\rho^2)$

$$=-2\sum_{n=1,2,\ldots}\rho^n\frac{\cos(nx)}{n}, \quad \rho^2<1. \tag{B.7}$$

Statement (I) follows after implicit differentiation of $\tan(\gamma)$.

To prove (II), one integrates (I) as

$$\begin{aligned} y &\equiv F(x,\rho) \\ &= (1-\rho^2)\int_0^x \mathrm{d}u\,\frac{1}{1+\rho^2-2\rho\cos(u)} \\ &= 2\arctan\left[\frac{1-\rho}{1+\rho}\tan(x/2)\right], \end{aligned} \tag{B.8}$$

which implies

$$(1+\rho)\tan[y/2]=(1-\rho)\tan[x/2], \tag{B.9}$$

and thus the symmetry $\{y\leftrightarrow x,\rho\leftrightarrow-\rho\}$.

Statement (III) is proved with the aid of (II):

$$\frac{\partial z}{\partial x}=\frac{\partial F(x,-\rho)}{\partial x}\equiv F'(x,-\rho). \tag{B.10}$$

On the other hand,

$$\begin{aligned} F'(z,\rho)\,\frac{\partial z}{\partial x} &\equiv \frac{\partial}{\partial x}F(z(x),\rho) \\ &\equiv \frac{\partial}{\partial x}F(F^{-1}(x,\rho),\rho)=1, \end{aligned} \tag{B.11}$$

which, together with (B.10) and (I), implies that

$$F'(z,\rho)=\frac{1}{F'(x,-\rho)}=\frac{1+\rho^2+2\rho\cos(x)}{1-\rho^2}. \tag{B.12}$$

Starting with (IVa), we have from (III) and (I)

$$\begin{aligned} F'(z,\rho) &= \frac{1+\rho^2+2\rho\cos(x)}{1-\rho^2} \\ &= \frac{1-\rho^2}{1+\rho^2-2\rho\cos(z)}, \end{aligned} \tag{B.13}$$

which, when solved for $\cos(z)$, gives (IVa). To show (IVb), one uses $\sin(z)=\pm\sqrt{1-\cos^2(z)}$ and fixes the sign by choosing a small positive x, which is connected with a positive z. The real and imaginary parts of (IV) are consistent with (IVa) and (IVb).

As to (V), one uses (I) and formula **1.447** 3. of [30]:

$$\begin{aligned} F'(x,\rho) &\equiv \frac{1-\rho^2}{1+\rho^2-2\rho\cos(x)} \\ &= 1+2\sum_{n=1,2,\ldots}\rho^n\cos(nx). \end{aligned} \tag{B.14}$$

Integration from zero to x proves (V).

Statement (VI) is proved similarly, this time with the aid of formula **1.447** 1. of [30]:

$$\begin{aligned} &\frac{\mathrm{d}}{\mathrm{d}x}\ln(1-2\rho\cos(x)+\rho^2) \\ &=\frac{2\rho\sin(x)}{1-2\rho\cos(x)+\rho^2}=2\sum_{n=1,2,\ldots}\rho^n\sin(nx). \end{aligned} \tag{B.15}$$

Integration from zero to x leads to

$$\begin{aligned} &\ln(1-2\rho\cos(x)+\rho^2)-2\ln(1-\rho) \\ &=-2\sum_{n=1,2,\ldots}\rho^n\frac{\cos(nx)}{n}+2\sum_{n=1,2,\ldots}\frac{\rho^n}{n}, \end{aligned} \tag{B.16}$$

where the latter sum is exactly equal to the constant term on the left-hand side.

C. Derivation of the Functional Equation for $W(\Phi)$

In this appendix we derive the integral equation (34) for $V(x)$ and its connection (36) with the distribution function $W(\Phi)$. The manipulations to follow are for a given wave number K, so the reflection coefficient ρ is a fixed parameter and will not be indicated as an independent variable. We start with the definition (32)

$$W_N(\Phi)=\frac{1}{N}\sum_{n=1}^{n}\delta_{\mathrm{per}}(\Phi-\Phi_n), \quad \Phi\in[-\pi,\pi), \tag{C.1}$$

and assume that $\lim_{N\to\infty}W_N$ is equivalent to the average with respect to the scatterer configurations. This amounts to average with respect to the independent random numbers $\varepsilon_1,\varepsilon_2,\ldots$:

$$W(\Phi)=\lim_{N\to\infty}\langle W_N(\Phi)\rangle_N, \tag{C.2}$$

where

$$\langle f\rangle_n=\int_{\mathbf{R}^n} f\,\mathrm{d}\varepsilon_1\mathrm{d}\varepsilon_2\ldots\mathrm{d}\varepsilon_n\,p(\varepsilon_1)p(\varepsilon_2)\ldots p(\varepsilon_n). \tag{C.3}$$

By the recurrence relation (23), the phase $\Phi_n \equiv \Phi_n(\varepsilon_1, \varepsilon_2, \ldots, \varepsilon_n)$ depends on the random numbers ε_i as follows:

$$\begin{aligned} \Phi_n &= 2\alpha\varepsilon_n + H_{n-1}, \\ H_{n-1} &= F(\Phi_{n-1}) - 2\alpha\varepsilon_{n-1} + \Omega, \\ H_0 &= \Omega - \theta + \sigma + \varphi_0, \end{aligned} \tag{C.4}$$

where H_{n-1} does not depend on the random number ε_n. This suggests to introduce the conditional probability density

$$U_N(x) = \frac{1}{N}\sum_{n=0}^{N-1} \langle \delta_{\mathrm{per}}(x - H_n)\rangle_n \tag{C.5}$$

to write

$$\langle W_N(\Phi)\rangle_N = \int_{\mathbf{R}} \mathrm{d}\varepsilon\, p(\varepsilon)\, U_N(\Phi - 2\alpha\varepsilon). \tag{C.6}$$

Both $U_N(x)$ and $W_N(x)$ are 2π-periodic in x and normalized to 1 in the interval $x \in (-\pi, \pi)$. In an ensemble of arrays with $n = 1, 2, \ldots, N$ scatterers, $U_N(\Phi - 2\alpha\varepsilon)$ is the average conditional probability density for the phase Φ with the last scatterer position of each array fixed.

We introduce an integral transform and a further reduction by the recursion (23):

$$\begin{aligned} &\langle \delta_{\mathrm{per}}(x - H_{\mathrm{n}})\rangle_{\mathrm{n}} \\ &= \int_{-\pi}^{\pi} \mathrm{d}y\, \langle \delta_{\mathrm{per}}(y - \Phi_n)\, \delta_{\mathrm{per}}(x - F(y) + 2\alpha\varepsilon_n - \Omega)\rangle_n \\ &= \int_{\mathbf{R}} \mathrm{d}\eta\, p(\eta) \int_{-\pi}^{\pi} \mathrm{d}y \langle \delta_{\mathrm{per}}(y - 2\alpha\eta - H_{n-1})\rangle_{n-1} \\ &\qquad \cdot \delta_{\mathrm{per}}(x - F(y) + 2\alpha\eta - \Omega). \end{aligned} \tag{C.7}$$

Since

$$U_N(x) = \frac{1}{N}\delta_{\mathrm{per}}(x - H_0) + \frac{1}{N}\sum_{n=1}^{N-1} \langle \delta_{\mathrm{per}}(x - H_n)\rangle_n, \tag{C.8}$$

where in the limit $N \to \infty$ one can neglect the first term, and after resummation $n - 1 \to n$, we obtain for large N

$$\begin{aligned} &U_N(x) = \\ &\int_{\mathbf{R}} \mathrm{d}\eta\, p(\eta) \int_{-\pi}^{\pi} \mathrm{d}y\, \frac{1}{N}\sum_{n=1}^{N-1} \langle \delta_{\mathrm{per}}(y - 2\alpha\eta - H_{n-1})\rangle_{n-1} \\ &\qquad \cdot \delta_{\mathrm{per}}(x - F(y) + 2\alpha\eta - \Omega) = \\ &\frac{N-1}{N} \int_{\mathbf{R}} \mathrm{d}\eta\, p(\eta) \int_{-\pi}^{\pi} \mathrm{d}y\, U_{N-1}(y - 2\alpha\eta) \\ &\qquad \cdot \delta_{\mathrm{per}}(x - F(y) + 2\alpha\eta - \Omega), \end{aligned} \tag{C.9}$$

and in the limit $N \to \infty$

$$\begin{aligned} &U(x) = \\ &\int_{\mathbf{R}} \mathrm{d}\eta\, p(\eta) \int_{-\pi}^{\pi} \mathrm{d}y\, \delta_{\mathrm{per}}(x - F(y) \\ &\qquad + 2\alpha\eta - \Omega)\, U(y - 2\alpha\eta). \end{aligned} \tag{C.10}$$

In order to carry out the y integration, it is first observed that, because of statement (I) of Appendix B, $F'(y) > 0$. Thus, the map $y \to F$ is one to one for all y; in particular $F(y)$ maps the interval $y \in [-\pi, \pi)$ onto it with $F(-\pi) = -\pi$ and $F(\pi) = \pi$. The zero $y = y^*$ of the argument of δ_{per} in (C.10) is unique. To see this, let us assume a further zero y^{**} with $(y^*, y^{**}) \in [-\pi, \pi)$. Then there exist integers r^* and r^{**} such that

$$\begin{aligned} &x - F(y^*) - \Omega + 2\alpha\eta + 2\pi r^* \\ &= x - F(y^{**}) - \Omega + 2\alpha\eta + 2\pi r^{**} \end{aligned} \tag{C.11}$$

or

$$F(y^{**}) - F(y^*) = 2\pi(r^{**} - r^*). \tag{C.12}$$

But since F maps the half-open interval $[-\pi, \pi)$ bijectively, we have $-2\pi < F(y^{**}) - F(y^*) < 2\pi$ which implies $r^{**} = r^*$; thus $F(y^{**}) = F(y^*)$ and $y^* = y^{**}$. On the other hand, since F is onto $[-\pi, \pi)$, one zero exists. The y integration in (C.10) now immediatley leads to the integral equation

$$\begin{aligned} U(x) &= \int_{\mathbf{R}} \mathrm{d}\eta\, p(\eta)\, \frac{1}{F'(y^*)}\, U(y^* - 2\alpha\eta), \\ y^* &= F^{-1}(x + 2\alpha\eta - \Omega), \end{aligned} \tag{C.13}$$

$$W(x) = \int_{\mathbf{R}} \mathrm{d}\varepsilon\, p(\varepsilon)\, U(x - 2\alpha\varepsilon). \tag{C.14}$$

Now we introduce the cumulative density (conditional probability function)

$$V(x) = \int_{-\pi}^{x} \mathrm{d}y\, U(y). \tag{C.15}$$

By definition, and because of the normalization and periodicity of U, it has the properties

$$\begin{aligned} &V(-\pi) = 0, \quad V(\pi) = 1, \\ &V(x + 2\pi) = V(x) + 1. \end{aligned} \tag{C.16}$$

To obtain an integral equation for V, one integrates (C.13) with respect to x and introduces on the right-hand side the one to one transformation

$$x \to y^* \equiv F^{-1}(x + 2\alpha\eta - \Omega). \tag{C.17}$$

We differentiate the relation $F(y^*(x)) = x + 2\alpha\eta - \Omega$ and introduce the notation $Y(x) \equiv y^*(x)$ to obtain $\mathrm{d}x = \mathrm{d}Y\,F'(Y)$ which leads to the integral equation

$$V(x) = \int_{\mathbf{R}} \mathrm{d}\eta\, p(\eta)\,[V(Y) - V(Y_0)] \tag{C.18}$$

with $Y(x) = F^{-1}(x - 2\alpha\eta - \Omega)$ and $Y_0 = Y(x = -\pi)$.

Finally, for the connection between V and W, one integrates the right-hand side of (C.14) partially with respect to ε and exploites that $p(\varepsilon)$ has finite support:

$$\begin{aligned} W(x) &= -\int_{\mathbf{R}} \mathrm{d}\varepsilon\, p'(\varepsilon) \int_{\varepsilon_0}^{\varepsilon} \mathrm{d}\eta\, U(x - 2\alpha\eta) \\ &= \frac{1}{2\alpha} \int_{\mathbf{R}} \mathrm{d}\varepsilon\, p'(\varepsilon) \int_{-\pi}^{x-2\alpha\varepsilon} \mathrm{d}y\, U(y), \\ W(x) &= \frac{1}{2\alpha} \int_{\mathbf{R}} \mathrm{d}\varepsilon\, p'(\varepsilon)\, V(x - 2\alpha\varepsilon). \end{aligned} \tag{C.19}$$

D. $W(\Phi)$ in the Regular Lattice Case

The disorder distribution is now $p(\varepsilon) = \delta(\varepsilon)$, which reduces (C.14) and (C.13) to $W(x) = U(x)$ and

$$\begin{aligned} &W_{\mathrm{reg}}(x) = \frac{1}{F'(Y)}\, W_{\mathrm{reg}}(Y), \\ &Y(x) = F^{-1}(x - \Omega). \end{aligned} \tag{D.1}$$

This functional equation has a simple solution:

$$W_{\mathrm{reg}}(x) = \delta(x - x^*), \quad F(x^*) = x^* - \Omega, \tag{D.2}$$

where x^* is a fixed point with $Y = x^*$, or $F(x^*) = x^* - \Omega$, which implies $F'(Y(x^*)) = 1$.

As it turns out, there exist two fixed points, but within band gaps only, which are characterized by the condition (see also p. 148 of [31])

$$\cos^2(\Omega/2) > \tau^2 \;\text{ or }\; \rho^2 > \sin^2(\Omega/2). \tag{D.3}$$

Clearly, among the two existing fixed points, the stable one has to be taken.

For band energies the situation is more involved. We solved the eigenvalue problem of the transfer matrix $M_n \equiv M_1$ with $\zeta_n \equiv 1$. The initial amplitude vector $\{a_0, b_0\}$, taken on the unit circle, was expressed in terms of the eigenvectors $\mathbf{e}_1, \mathbf{e}_2$. The matrix power then has the structure

$$(M_1)^n = c\,\exp[\mathrm{i}n\lambda]\mathbf{e}_1 + d\,\exp[-\mathrm{i}n\lambda]\mathbf{e}_2 \tag{D.4}$$

with the complex constants c, d expresssed in terms of the initial phase $a_0/b_0 = \exp[\mathrm{i}\varphi_0]$ and components of the eigenvectors. The decisive point now is that, according to Jacobi's theorem [27], the phases $\phi_n \equiv n\lambda$, $n = 1, 2, \ldots$, cover the unit circle densely and uniformly with distribution $W(\phi) = 1/(2\pi)$, provided $\lambda = \lambda(K)$ is irrational modulo (2π), which is the case for almost all wave numbers K. The constant distribution of ϕ has to be transformed to the distribution of the phases φ_n of $a_n/b_n = \exp[\mathrm{i}\varphi_n]$. Omitting details, we give the final result in terms of the phase $\Phi = \varphi + \theta + \sigma$, see (22):

$$\begin{aligned} &W_{\mathrm{reg}}(\Phi) = \frac{1}{2\pi}\, \frac{\sqrt{1 - R^2}}{1 + R\sin(\Phi - \Omega/2)}, \\ &R = \frac{\rho}{\sin(\Omega/2)}, \quad R^2 < 1. \end{aligned} \tag{D.5}$$

One can show that

$$\begin{aligned} &\int_{-\pi}^{\pi} \mathrm{d}\Phi\, W_{\mathrm{reg}}(\Phi)\;\; \ln(1 - 2\rho\cos(\Phi) + \rho^2) \\ &= \ln(1 - \rho^2), \end{aligned} \tag{D.6}$$

which ensures that the Lyapunov exponent, see (33), is exactly zero.

In the following we prove that W_{reg} fulfills the functional equation (D.1). We use statements (III), (IVa), and (IVb) of Appendix B to write

$$\begin{aligned} &\frac{1}{F'(Y(x))} = \frac{1 - \rho^2}{1 + \rho^2 + 2\rho\cos(x - \Omega)}, \\ &Y(x) = F^{-1}(x - \Omega), \end{aligned} \tag{D.7}$$

$$\begin{aligned} \cos(Y) &= \frac{2\rho + \cos(x - \Omega) + \rho^2\cos(x - \Omega)}{1 + \rho^2 + 2\rho\cos(x - \Omega)}, \\ \sin(Y) &= \frac{(1 - \rho^2)\sin(x - \Omega)}{1 + \rho^2 + 2\rho\cos(x - \Omega)}. \end{aligned} \tag{D.8}$$

We insert (D.5) and (D.7) into (D.1), introduce the abbreviation $\omega = \Omega/2$, and solve for $\sin(Y - \omega)$, which appears on the right-hand side of (D.1):

$$\begin{aligned} &\sin(Y - \omega) = \big[-2\rho\sin(\omega) - 2\cos(x - 2\omega)\sin(\omega) \\ &+ \sin(x - \omega) - \rho^2\sin(x - \omega)\big]\big[1 + \rho^2 \\ &- 2\rho\cos(x - 2\omega)\big]^{-1} = \big[-2\rho\sin(\omega) + \sin(x - 3\omega) \\ &- \rho^2\sin(x - \omega)\big]\big[1 + \rho^2 - 2\rho\cos(x - 2\omega)\big]^{-1}, \\ &\omega = \Omega/2. \end{aligned} \tag{D.9}$$

In the next step, we write the left-hand side of (D.9) as

$$\sin(Y-\omega) = \sin(Y)\cos(\omega) - \cos(Y)\sin(\omega), \quad \text{(D.10)}$$

and insert the expressions given in (D.8). After elementary trigonometric manipulations, one recovers exactly the right-hand side of (D.9), which proves that W_{reg} fulfills the functional equation (D.1).

Acknowledgement

The author is very much indepted to Jürgen Parisi for his support and encouragement, and for a critical reading of the manuscript. He is also thankful to the referees for their constructive comments which were helpful for the final version of the manuscript.

[1] L. Avgin, Phys. Rev. B **73**, 052201 (2006).
[2] H. Cheraghchi, S. M. Fazeli, and K. Esfarjani, Phys. Rev. B **72**, 174207 (2005).
[3] T. Sedrakyan and A. Ossipov, Phys. Rev. B **70**, 214206 (2004).
[4] T. Sedrakyan, Phys. Rev. B **69**, 085109 (2004).
[5] L. Sanchez-Palencia, D. Clément, P. Lugan, P. Bouyer, G. V. Shlyapnikov, and A. Aspect, Phys. Rev. Lett. **98**, 210401 (2007).
[6] Y. Xiong, Phys. Rev. **75**, 073411 (2007).
[7] S. Kotani and B. Simon, Comm. Math. Phys. **112**, 103 (1987).
[8] P. Stollmann, Caught by Disorder, Birkhäuser, Boston 2001.
[9] P. W. Anderson, Phys. Rev. **109**, 1492 (1958).
[10] E. Abraham, P. W. Anderson, D. C. Licciardello, and T. V. Ramakrishnan, Phys. Rev. Lett. **42**, 673 (1979).
[11] D. Vollhardt and P. Wölfle, Phys. Rev. Lett. **48**, 699 (1982).
[12] P. A. Lee and T. V. Ramakrishnan, Rev. Mod. Phys. **57**, 287 (1985).
[13] J. T. Edwards and D. J. Thouless, J. Phys. C: Solid State Phys. **5**, 807 (1972).
[14] M. Weissmann and A. M. Llois, Phys. Rev. B **41**, 10191 (1990).
[15] M. Schreiber and H. Grussbach, Phys. Rev. B **67**, 607 (1991).
[16] P. Phillips, Annu. Rev. Phys. Chem. **44**, 115 (1993).
[17] H. Yamada and T. Okabe, Phys. Rev. E **63**, 026203-1 (2001).
[18] M. Hjort and S. Stafström, Phys. Rev. B **62**, 5245 (2000).
[19] P. Lloyd, J. Phys. C **2**, 1717 (1969).
[20] L. I. Deych, D. Zaslavsky, and A. A. Lisyansky, Phys. Rev. E **64**, 224202 (2001).
[21] J. Heinrichs, Phys. Rev. B **66**, 1554348 (2002).
[22] R. Sims and G. Stolz, Commun. Math. Phys. **213**, 575 (2000).
[23] I. Y. Gol'dsheid and G. A. Margulis, Russian Math. Surveys **44**, 11 (1989).
[24] H. Furstenberg, Trans. Am. Math. Soc. **108**, 377 (1963).
[25] D. Ruelle, Ann. Math. **115**, 243 (1982).
[26] H. Schmidt, Phys. Rev. **105**, 425 (1957).
[27] R. L. Devaney, Chaotic Dynamical Systems, 2nd ed., Addison-Wesley, Redwood City 1989.
[28] Mathematica Version 6.0.2.0, Wolfram Research, Champaign, IL, USA 2007.
[29] F. Schwabl, Quantenmechanik, 3rd ed., Springer, Berlin 1992.
[30] I. S. Gradshteyn and I. M. Ryzhik, Table of Integrals, Series, and Products, 4th ed., Academic Press, New York 1965.
[31] N. W. Ashcroft and N. D. Mermin, Solid State Physics, Saunders College Publishing, Fort Worth 1976.